USING REMOTE SENSING TO MAP THE DISTRIBUTION OF SAGO PALMS IN NORTHEASTERN MINDANAO, PHILIPPINES: RESULTS BASED ON LANDSAT ETM+ IMAGE ANALYSIS

Jojene R. SANTILLAN[a], Meriam M. SANTILLAN[b], Richelle FRANCISCO[a]

[a] Research Laboratory for Applied Geodesy and Space Technology, Training Center for Applied Geodesy and Photogrammetry & Department of Geodetic Engineering, University of the Philippines, Diliman, Quezon City, Philippines; Tel: +63-2-9818500 ext. 3147; E-mail: jrsantillan@up.edu.ph

[b] Division of Geodetic Engineering, College of Engineering and Information Technology, Caraga State University, Ampayon, Butuan City, Philippines; Tel: +63-85-3412296; E-mail: mmsantillan@carsu.edu.ph

KEY WORDS: Sago palm, Landsat ETM+, Agusan del Sur, Mindanao, Philippines.

ABSTRACT: We present in this paper the results of our study that aims to map the distribution of the sago palm (*Metroxylon sagu*) in Agusan del Sur province in northeastern Mindanao, Philippines using remote sensing data and techniques. The sago palms have been reported to exist in marshlands and wetlands of northeastern Mindanao which are difficult to access and would be costly if mapped using conventional field mapping techniques. We tested the viability of Landsat ETM+ image to locate the distribution and abundance of the sago palm in the Agusan del Sur province. After radiometric calibration and atmospheric correction, the image was subjected to Maximum Likelihood classification to produce a land cover map showing the distribution of sago palms and other land-cover types. The classifier was trained and the accuracy of the results assessed using ground truth data of sago palm and other land-cover types that were collected between February and August 2012. Results of the supervised classification using combination of all the multispectral bands, NDVI and SRTM DEM showed an overall classification accuracy of 94.88%. A total of 597 hectares of sago palms were detected from the image analysis. The sago palm classification has 80.18% Producer's Accuracy and 82.66% User's Accuracies. This relatively low Producer and User's Accuracies of the sago palm classification may be attributed to three factors: (i) the similarities in the spectral characteristics of sago palm with other palm vegetation, especially coconut and oil palm; (ii.) the 30-m spatial resolution of the Landsat ETM+ image may not be optimal for classifying specific vegetation species such as the sago palms, especially in areas where sago palms are interspersed with other land-cover types; and (iii.) the differences in the date of image acquisition and the date of field surveys when the sago ground truth data were collected. Despite these low accuracies for sago palms, the location, extent and distribution of sago palms depicted in the derived land-cover map provides vital information as to where sago palms are deemed to be abundant in Agusan del Sur province.

INTRODUCTION

The sago palm (*Metroxylon sagu Rottb.*), as shown in Figure 1, is well known for its rich starch contents (Flach, 1997) and as a significant source of other raw materials of high economical value (Abd-Aziz, 2002). Interests in this palm species has increased considerably in the last 3 decades because of its advantages of being economically acceptable, relatively sustainable, environmentally friendly, uniquely versatile, vigorous, and promotes socially stable agroforestry systems (Flach, 1997; Stanton, 1993).

In the Philippines, the sago palm has recently gained interest, especially for its commercial utilization being a significant source of starch that can be converted into flour, lactic acid, ethanol and biodegradable plastics. However, information on its present location and distribution is missing, and it cannot be ascertained whether there is enough supply of sago to drive and sustain a large scale sago starch industry. The sago palms have been reported to exist in marshlands and wetlands of northeastern Mindanao which are difficult to access and would be costly if mapped using conventional field mapping techniques. Therefore, the use of remote sensing (RS) data and techniques would be appropriate for this purpose.

Figure 1: The sago palm in clusters (a), and as an individual tree (b).

While several studies have been reported to have used remote sensing techniques in mapping forest resources and agricultural crops (e.g., Boyd & Danson, 2005; Pinter, at al., 2003), nothing have been published so far that relates to the use of appropriate techniques in mapping the distribution of the sago palm. All literatures pertaining to the location, extent and distribution of sago palms are indicative of using conventional field survey mapping methods (e.g., Josue & Okazaki, 2002).This situation opens up several opportunities for the adoption of existing RS-based techniques as starting point for mapping of the sago palm in RS images, which could lessen logistical and practical difficulties that are often encountered when using conventional field surveys, especially in inaccessible areas.

The objective of this study is to test the viability of Landsat ETM+ image in mapping the distribution and abundance of the sago palms. Existing supervised classification algorithms coupled with ground truth surveys are utilized to map the sago palms in the image.

METHODS

The test study area is the province of Agusan del Sur in northeastern Mindanao, Philippines (Figure 2). It has been reported that tracts of sago palms exist in this area but no information is available on the overall actual location and extent of the sago areas.

The steps employed in the detection of sago palms in the Landsat ETM+ image are shown in Figure 3. The steps are discussed in the next sections.

The Landsat ETM+ image

The Landsat ETM+ satellite image of the test study area (Figure 2) was acquired on September 14, 2008. A GeoTIFF format of this image was downloaded online through the USGS Global Visualization Viewer (GLOVIS, http://glovis.usgs.gov). Recent images acquired by the Landsat ETM+ sensor for Eastern Mindanao are also available for download from the GLOVIS website. However, these more recent images are heavily contaminated by clouds and shadows, making it almost impossible to generate a more informative land-cover map. Through visual inspection, the image acquired on September 14, 2008 was selected for analysis due to the less contamination of clouds and shadows. Unfortunately, there are also missing information in this image due to gaps during image acquisition brought about by the failure of the Scan Line Corrector of the ETM+ sensor.

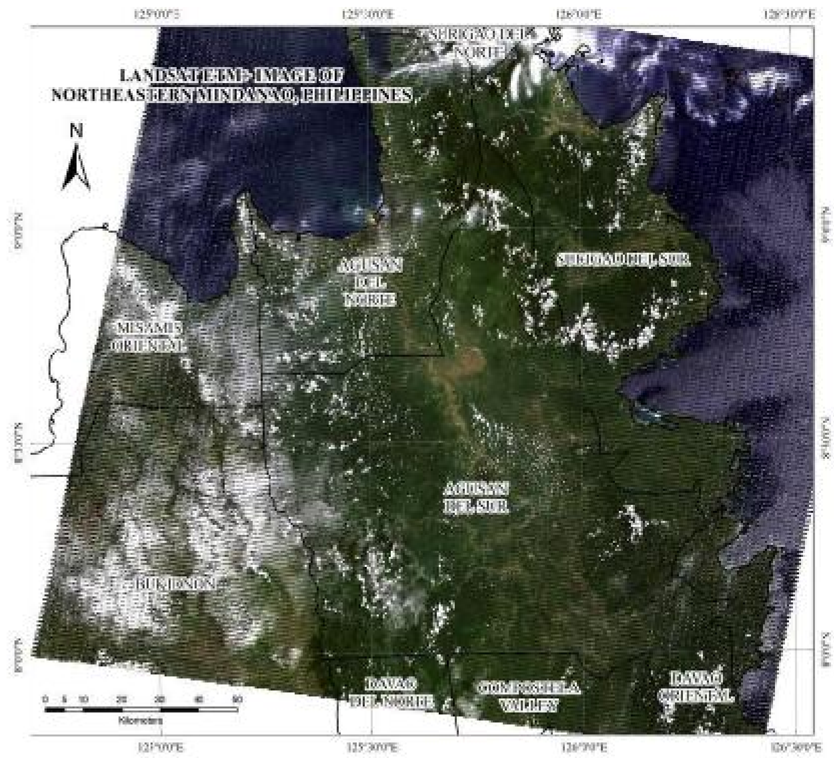

Figure 2: The Landsat ETM+ image of northeastern Mindanao (displayed in true color) acquired on September 14, 2008. The test study area, Agusan del Sur province, is shown in this map.

Pre-processing steps were applied to the Landsat ETM+ image to enhance its interpretability and to correct it from atmospheric effects. This includes radiometric calibration to convert the DN values to top-of-atmosphere reflectance (TOA) using the Landsat calibration equations. A fast atmospheric correction by means of the dark-object subtraction method using band minimum (Schowengerdt, 1997) was applied to the TOA reflectance image. A further nominal calibration using a standard atmospheric model was not done because the necessary input data and software facilities for such model were not available during the conduct of image calibrations.

Normalized Difference Vegetation Index (NDVI) and a resampled SRTM DEM were added to increase the number of bands during image classification. The SRTM DEM was added as it has been found that addition of DEMs increases classification accuracy especially in areas of rugged terrain (Elumnoh & Shrestha, 2000).

To minimize the error and confusion that cloud cover and shadows may introduce to the extraction of land-cover information during the image classification process, manual digitizing of these features in the image was done. A cloud-and-shadow mask was then created and used to clean the image before the image classification.

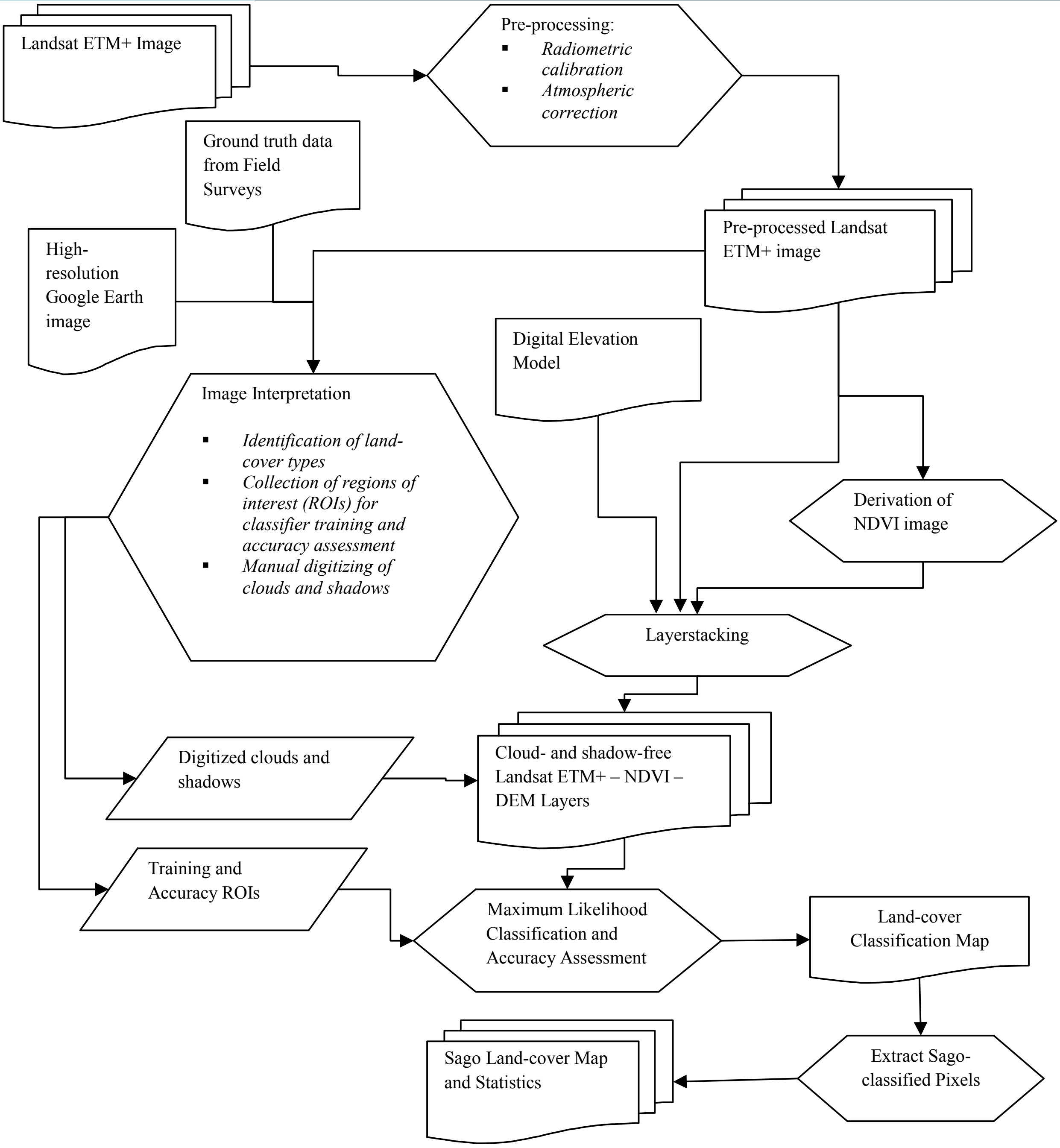

Figure 3: Process flow diagram of Landsat ETM+ image analysis to map sago palms

Image Interpretation and Selection of Samples for Classifier Training and Accuracy Assessment

The pre-processed Landsat ETM+ image was visually interpreted to obtain information as to what land-cover types are present in the study area. Several color composites were created to adequately identify the various land-cover types. In addition to this, high resolution images provided by the Google Earth application were also used as references to aid the interpretation. Data from field surveys conducted between February – August 2012 in the study area were used as guide in identifying sago palms and other land-cover types in the image. A total of thirteen (13) land-cover types were identified (Table 1).

Upon the recommendation of Jensen (1996), representative groups of pixels (or Regions of Interests, ROIs) were collected for each land-cover type that will be used for training the classifier. For each class, a practical minimum of 10**N* (where *N* = number of input bands) pixels were collected in order to have as many training pixels as possible that will ensure proper estimation of the parameters of the Maximum Likelihood classifier, as well as to ensure that its normal assumption of normal distribution is satisfied. For accuracy assessment, an independent set of pixels for each land-cover types were also collected from the image prior to the actual classification (hereafter referred to as "Accuracy Assessment Pixels, AAP"). Reference datasets such as Google Earth images were used extensively to ensure that each pixel collected from the Landsat ETM+ image is correctly identified as belonging to a particular land-cover type. This is further assisted by data gathered from the field surveys, especially in the case of sago palms. For each land-cover type, it was ensured that total number of collected AAP is at least 50 upon the recommendation of Congalton & Green (1999). Table 2 summarizes the number of pixels collected for classifier training and accuracy assessment.

Table 1. Land-cover types identified in the Landsat ETM+ image.

Land-cover type	Description
Barren Lands	Denuded mountain areas, bare exposed soils (other than croplands). Also include unpaved roads.
Built-up Areas	Residential, commercial and industrial areas as well as other man-made features such as roads and bridges, majority of which have impervious surfaces.
Cropland	Comprised of areas used for agriculture and planting of crops (includes planted/unplanted ricefields)
Dense vegetation	Densely vegetated areas, especially of the vegetation type found in forested areas (e.g., wooded vegetation). Also includes trees planted in parks and recreational areas, in residential areas and along the road. This type does not include grasslands.
Exposed River Bed	Exposed rocks, sands, stones, cobbles, and boulders along rivers and streams that are not covered by water during the time of image acquisition.
Grasslands	Areas where the vegetation is dominated by grasses and other herbaceous (non-woody) plants
Mangroves	Tract of lands covered by mangrove forests.
Palm - Banana	Tract of lands planted with bananas.
Palm - Coconut	Tract of lands planted with coconut trees.
Palm - Nipa	Tract of lands where nipa grows.
Palm – Oil Palm	Tract of lands planted with oil palm
Palm - Sago Palm	Tract of lands where sago palms can be found (either planted or in the wild)
Water	Seas, lakes, reservoirs, rivers and streams.

Table 2. Number of pixels collected for classifier training and accuracy assessment.

Land-cover Type	Number of Pixels (30x30 m)	
	Training	Accuracy Assessment
Barren Lands	2,160	537
Built-up Areas	2,444	604
Cropland	5,589	1,391
Dense Vegetation	14,682	3,671
Exposed River Bed	452	114
Grassland	1,851	456
Mangroves	1,762	440
Palm - Banana	1,324	332
Palm - Coconut	1,038	240
Palm - Nipa	465	18
Palm – Oil Palm	9,620	2,336
Palm - Sago Palm	721	333
Water	11,123	2,493
Total	53,321	12,965

Maximum Likelihood Classification and Accuracy Assessment

The Maximum Likelihood classifier (MLC) is a parametric classifier based on statistical theory with the assumption that spectral signatures of the land-cover classes are normally distributed (Swain & Davis, 1978). MLC quantitatively evaluates both the variance and covariance of the class spectral signatures (Shalaby & Tateishi, 2007) and based on the evaluation, discriminant functions for each class are developed and used to classify an unknown pixel. A thorough discussion of the MLC can be found in Richards & Jia (1999). The MLC has been widely used in land-use/land-cover classification of remotely sensed images (Shalaby and Tateishi, 2007).

In this study, the MLC was trained and used to classify the several combinations of the 6 Landsat ETM+ bands, NDVI, and SRTM DEM. After each classification, a 3x3 majority analysis was employed to smoothen the classification results. Then, error matrices detailing the accuracy of the classification for each combination were prepared by comparing the AAP with the classification results. Three measures of accuracy were employed to test the classified images, namely the *Overall Classification Accuracy* (in percent), *Producer's Accuracy* (PA) and *User's Accuracy* (UA).

RESULTS AND DISCUSSIONS

The Classified Landsat ETM+ Image

Table 3 summarizes the results of the Maximum Likelihood Classification of the image bands, ratios, NDVI and DEM combinations (shown in Figure 4). The accuracy was assessed after applying a majority analysis of the classified image. It is worth mentioning that the addition of the SRTM DEM in the classification increased the classification accuracy.

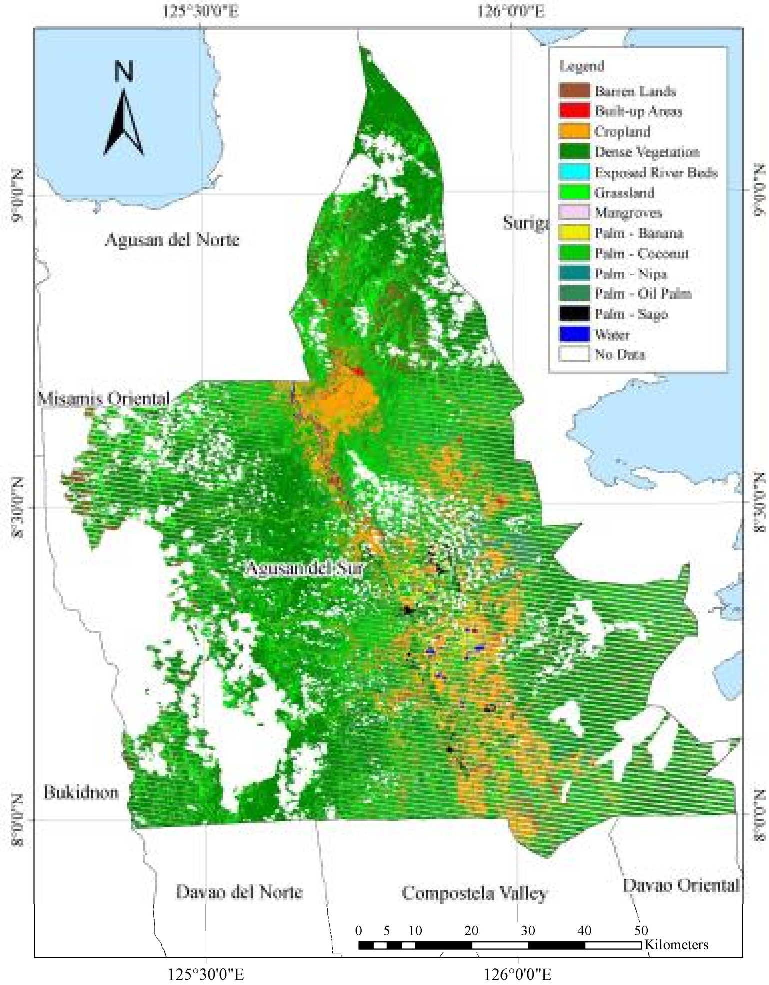

Figure 4: The land-cover map of Agusan del Sur derived from the Maximum Likelihood classification of combination of all the 6 multispectral bands of Landsat, NDVI and SRTM DEM

Table 3. Summary of Overall Classification, Producer's, and User's Accuracy of the Maximum Likelihood Classification of the Landsat ETM+ image.

Input Band Combinations	Overall Classification Accuracy (%, out of 12,965 samples)	Sago Palm Producer's Accuracy (%, out of 333 samples)	Sago Palm User's Accuracy (%, out of 233 samples)
All multispectral bands (1, 2, 3, 4, 5 & 7)	91.68	68.41	66.76
All multispectral bands + NDVI	91.05	70.31	60.34
All multispectral bands + DEM	95.14	79.59	83.54
All multispectral bands + NDVI + DEM	94.88	80.18	82.66

Among the 4 combinations, the classification using all the 6 multispectral bands + NDVI + DEM combination gained the highest PA of 80.18% for sago palm. On the other hand, the classification using all the 6 multispectral bands + DEM combination gained the highest UA for sago palm (83.54%). The results showed that the two combinations produce different results in terms of PA and UA. Also, the overall classification accuracy is higher for the 6 multispectral bands + DEM combination. However, in this study, the classification result using the 6 multispectral bands + NDVI + DEM combination was selected as PA and UA for sago palm surpassed the 80% mark. The map of the detected sago palms is shown in Figure 5.

The classification error matrix (Table 4) shows that out of the 333 AAP for sago palms, only 267 (or 80.18%) were classified correctly. The remaining 66 pixels (or a 19.82% error of omission) were not classified as sago palms but classified as other land-cover types. Majority of these pixels are classified as coconut palms. The User's Accuracy may provide indication that there is 82.66% probability that the classified sago palms in the land-cover map actually represent the sago palms as they occur on the ground. In this case, the classification of sago palms incurred a commission error of 17.34%. Looking at the error matrix, it can be observed that on a sample of 233 pixels classified as sago palms, only 267 of these were actually sago palms. The remaining 56 are other land-cover types that were falsely classified as sago palms.

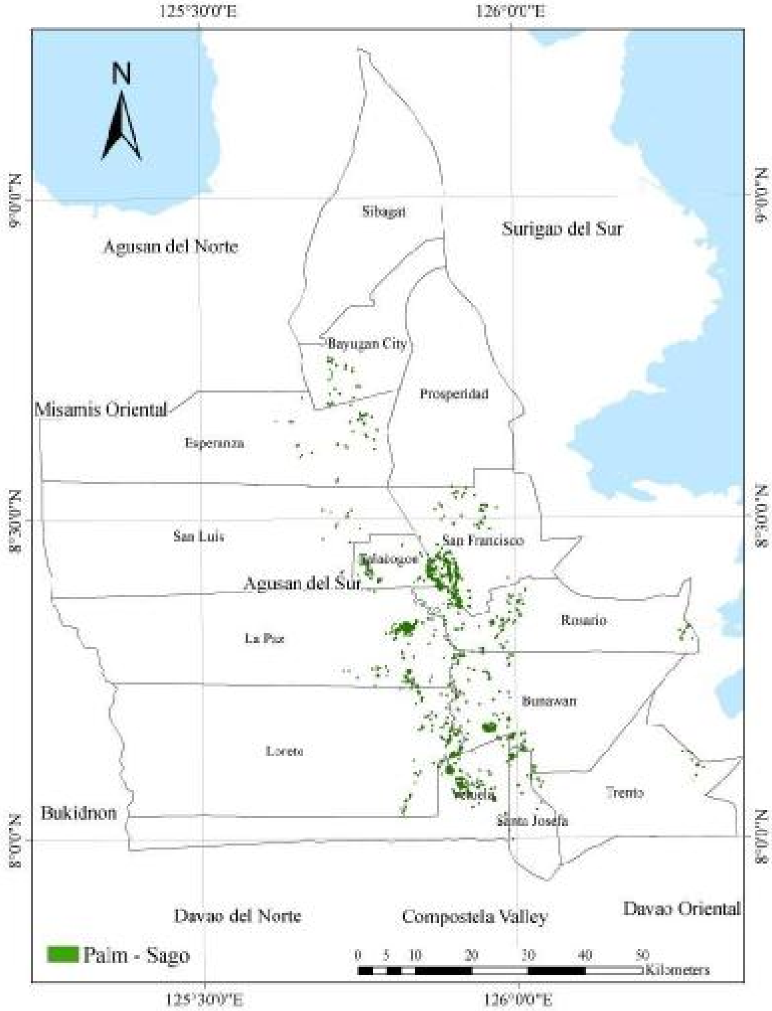

Figure 5: Map showing the location of the detected sago palms in the Agusan del Sur province.

The low accuracies of the sago palm classification may be attributed to three factors:

1. The similarities in the spectral characteristics of sago palms with other palm vegetation, especially coconut and oil palm. The error matrix shows that 49 of sago palm were classified as coconut. Likewise, 21 coconut and 30 oil palm pixels were erroneously classified as sago palms. This may indicate that spectral information derived from the sago, coconut and oil palm samples selected for classifier training could not provide adequate statistics in such a way that each of these land-cover types could be easily separated from each other in the image. The use of more number of training samples for these land-cover types may be a solution to this problem.
2. In areas where sago palms are interspersed with other land-cover types (which are common in areas visited during the field surveys), the 30-m spatial resolution of the Landsat ETM+ image may not be optimal for classifiying the sago palms, especially. The pixel size of 30-m x 30-m is large enough for several land-cover types to exist. Hence, no matter how accurate the position of a sago stand is obtained during the field surveys for use in accuracy testing as long as a sago stand is less than 30-m x 30-m in area, this point may not be reflected as sago palms in the classified image but the dominant land-cover type where the sago palms are located.
3. The differences in the date of image acquisition and the date of field surveys when the sago ground truth data were collected. Some of the sago palms mapped during the field surveys may have been recently grown and have not yet existed in the September 14, 2008 (the date of image acquisition). This creates a big contribution in lowering the Producer's Accuracy of the sago palms.

Table 4. The error matrix of the classification using the combination of all the 6 multispectral bands of Landsat, NDVI and SRTM DEM.

	Land-cover Types	*Accuracy Assessment/Ground Truth Pixels (AAP)*													
		Barren lands	Built-up Areas	Crop-land	Dense Vegetation	Exposed River Beds	Grass-land	Mangroves	Palm - Banana	Palm - Coconut	Palm - Nipa	Palm – Oil Palm	Palm - Sago	Water	Total
Classified Pixels	Barren lands	**511**	10	23	0	1	0	0	0	0	0	0	0	0	545
	Built-up Areas	0	**571**	13	0	7	1	0	0	2	0	0	3	1	598
	Cropland	23	10	**1345**	0	0	0	14	3	2	3	1	11	20	1432
	Dense Vegetation	0	0	0	**3504**	0	0	2	0	6	0	76	0	0	3588
	Exposed River Beds	0	13	0	0	**106**	0	0	0	0	0	0	0	0	119
	Grassland	1	0	0	69	0	**451**	0	0	11	0	21	1	0	554
	Mangroves	0	0	0	0	0	0	**398**	1	13	8	0	1	0	421
	Palm - Banana	0	0	1	0	0	0	1	**321**	8	0	0	0	0	331
	Palm - Coconut	2	0	6	16	0	3	13	4	**170**	0	29	49	0	292
	Palm - Nipa	0	0	1	0	0	0	10	0	6	**6**	0	0	0	23
	Palm – Oil Palm	0	0	0	82	0	1	0	0	1	0	**2179**	1	0	2264
	Palm - Sago	0	0	0	0	0	0	2	3	21	0	30	**267**	0	323
	Water	0	0	2	0	0	0	0	0	0	1	0	0	**2472**	2475
	Total	537	604	1391	3671	114	456	440	332	240	18	2336	333	2493	**12,965**

Detected Sago Palms in Agusan del Sur

The estimated area (in hectares) of the detected sago palms in each municipality of Agusan del Sur is shown in Figure 6. The sago palm areas are plotted with error bars indicating uncertainties due to omission and commission errors of the classification.

According to the result of the 2008 Landsat ETM+ image analysis, a total of 597 hectares of sago palms were estimated to exist in the Agusan del Sur province. The classification results indicate that sago palms are most abundant in the municipalities of San Francisco (139 hectares), followed by La Paz (112), Talacogon (102), Veruela (88), Rosario (72), and Bunawan (40).

Aside from the uncertainties associated with the commission and omission errors, care should be taken when using the estimated sago palm areas. It can be recalled that there are missing information in the image due to gaps during image acquisition brought about by the failure of the Scan Line Corrector of the ETM+ sensor. This is in addition to the clouds and shadows that were removed prior to the classification. Hence, the computed statistics may be considered underestimated.

It must be stated also that the detection of a relatively large area of sago palms in the municipalities of San Francisco and Talacogon municipalities is considered to be a discovery in this study that needs to be validated. No ground truth data on sago palms were collected in these municipalities.

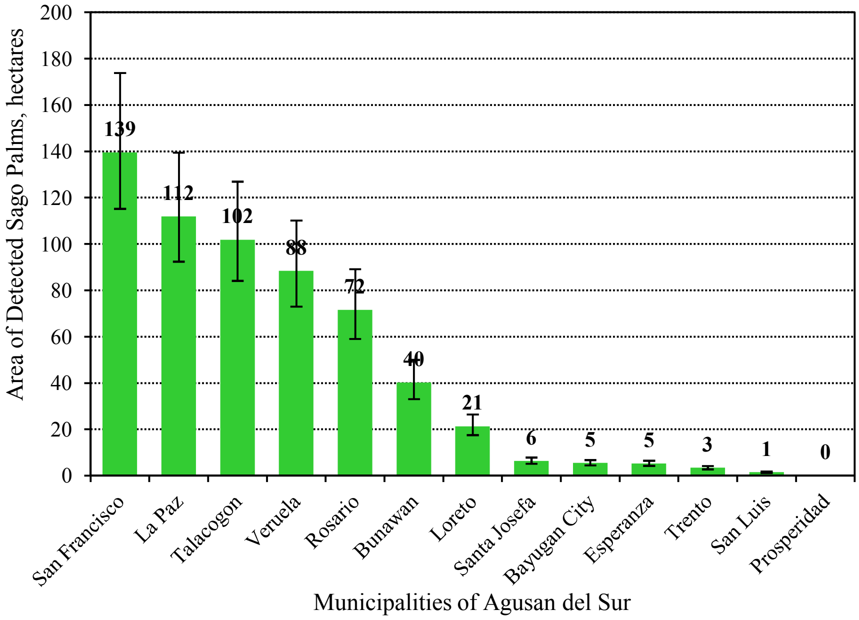

Figure 6: Area of sago palms detected from Maximum Likelihood classification of a combination of the 6 multispectral bands of Landsat, NDVI and SRTM DEM. A total of 705 hectares of sago palms were detected. Error bars indicate uncertainties in the classification of the sago palms. Lower error bars represents errors of commission while the upper bars represent errors of omission.

CONCLUSIONS

In this study we tested the viability of Landsat ETM+ image in mapping the distribution and abundance of the sago palm, focusing in the province of Agusan del Sur in northeastern Mindanao, Philippines. The sago classification results showed an above 80% accuracy for detecting sago palms in the image. A total of 597 hectares of sago palms were detected in Agusan del Sur. Although the PA and UA of the detected sago palms did not reached the 85% accuracy standard, the classification approach implemented in this study shows that sago palms can be detected in Landsat ETM+ images with modest accuracy. The accuracy of the classification can be improved by increasing the number of ROIs during classifier training. Use and evaluation of other classification algorithms to detect the sago palms may be a subject of future research.

The location, extent and distribution of sago palms derived from the Landsat ETM+ image analysis provides vital information as to where sago palms are deemed to be abundant in Agusan del Sur province. The sago maps produced in this study may be used as basis to ascertain whether there is enough supply of sago to drive and sustain a large scale sago starch industry. Presently, the classification approach is implemented to map all existing sago palms in the remaining areas of Mindanao, Philippines using the latest Landsat ETM+ images.

ACKNOWLEDGEMENT

This work is one the outputs of two research projects funded by the Philippine Council for Industry, Energy and Emerging Technology Research and Development of the Department of Science and Technology (PCIEERD-DOST) namely, *Project II.3-Mapping Sago Habitats and Sago Suitable Sites using Optical and Radar Image Analysis and Suitability Relationships*, and *Project II.2-Biophysical, Structural and Spectral Characterization of the Sago Palm*. We thank the following personnel and students of the College of Engineering and Information Technology of the Caraga State University for their assistance during ground truth data collection namely, Engr.

Michelle V. Japitana, Engr. Arnold G. Apdohan, Arthur M. Amora, Linbert Cutamora, Dylan Dikraven Galavia and Cherry Bryan G. Ramirez. We also thank Dr.Nilo Oponda and Mr. Adrian Almeria of UP Mindanao for sharing sago palm ground truth datasets they collected in Agusan del Sur. The first author acknowledges the University of the Philippines-Diliman for the Research Dissemination Grant.

REFERENCES

Abd-Aziz, S., 2002. Sago starch and its utilization. Journal of Bioscience and Bioengineering, 94(6), pp. 526-529, 2002.

Boyd, D.S., Danson, F.M., 2005. Satellite remote sensing of forest resources: three decades of research development. Progress in Physical Geography, 29(1), pp. 1-26.

Congalton, R.G., Green, K., 199. Assessing the Accuracy of Remotely Sensed Data: Principles and Practices; Lewis Publishers: Boca Rotan, FL, USA, 1999.

Elumnoh, A., Shrestha, R.P., 2000. Application of DEM data to Landsat image classification: evaluation in a tropical wet-dry landscape of Thailand. Photogrammetric Engineering & Remote Sensing, 66(3), pp. 297-304.

Flach, M., 1997. Metroxylon sagu Rottb. - Promoting the conservation and use of underutilized and neglected crops. Institute of Plant Genetics and Crop Plant Research, Gatesleben/International Plant Genetic Resources, Rome, Italy.

Josue, A.R., Okazaki, M., 2002. Sago cultivation in Northern Mindanao, Philippines. Sago Palm, pp. 43-50.

Pinter, P.J., et al., 2003. Remote sensing for crop management. Photogrammetric Engineering & Remote Sensing, 69(6), pp. 647-664.

Richards, J.A., Jia, X., 1999. Remote Sensing Digital Image Analysis, Third Edition, Springer-Verlag: Berlin Heidelberg New York.

Schowengerdt, R.A., 1997. Remote Sensing: Models and Methods for Image Processing, Second Edition, Academic Press.

Shalaby, A., Tateishi, R., 2007. Remote sensing and GIS for mapping and monitoring land-cover and land-use changes in the Northwestern coastal zone of Egypt. Applied Geography, 27:28-41

Stanton, R., 1993. Perspective on, and future prospects for, the sago industry. Sago Palm, 1(1), pp. 2-7.

Swain, P.H., Davis, S.M. (Eds.), 1978. Remote Sensing: The Quantitative Approach, McGraw-Hill: New York.